CSI-Based WiFi-Inertial State Estimation

Bing Li, Shengkai Zhang and Shaojie Shen

***Abstract*— WiFi-based localization has received increasing attentions these years because WiFi devices are low-cost and universal. Recent years, tens of WiFi-based localization systems have been proposed which could achieve decimeter-level accuracy with the commercial NIC and with no specialized infrastructure. However, such systems require the positions of the Access Points or fingerprint map to be known in advance. In this paper, we present CWISE, an accurate WiFi-Inertial SLAM system without requirement for Access Points' positions, specialized infrastructure or fingerprinting. CWISE relies only on a commercial NIC with two antennas and an IMU. We test the CWISE system on a flying quadrotor and it shows that the system could work in real time and obtain mean accuracy of 1.60m.**

I. INTRODUCTION

State estimation is the fundamental requirement for many robotic applications such as UAV, self-driving car. A large number of researchers have proposed various state estimation methods using laser scanner [1] [2], stereo cameras[3] [4], monocular camera[5] [6] [7], and RGB-D sensors[8]. Laser-based methods could achieve centimeter level accuracy at indoor environments, but they are limited by the requirement for expensive laser sensor. Vision-based approaches obtain great success due to the property of low cost, high accuracy and light weight, however, they require sufficient lighting and features, they do not work at dark or featureless environments. While WiFi-based approaches could potentially solve these problem, because WiFi devices are cheap, universal and unaffected by the light or feature.

The main goal of this paper is to develop a WiFi-based localization system that is:

- deployable: The system should be easily deployed on existing commodity WiFi infrastructure without requiring any hardware change to the access points(APs)
- accurate: The system should be as accurate as comparable with GPS to be used for autonomous flight of aerial robots.
- on-the-fly: The system should be always ready to fly without any preparing work when changes to a different place, for example, no need to measure the positions of the APS and no need to build the fingerprint map of the WiFi signal.

To the best of our knowledge, there is no WiFi-based system satisfying all these three properties. RSSI based systems are easily deployable but are not accurate, their accuracy ranges from 2-4 m [9] which is not sufficient for robotic navigation. Recent methods that based on angle of arrival (AoA) estimation such as ArrayTrack [10] and Phaser [11] are accurate but they need to modify the hardware to get a multiple antennas (5-8) system. Other AoA-based approaches such as Ubicarse [12] and SpotFi [13] are deployable and accurate, but they cannot be used on highly dynamic system. Additionally, all these approaches above need to know the positions of APs in advance, they are not on-the-fly.

The main contribution of this paper is a real time WiFi-Inertial state estimation system which is deployable, accurate and on-the-fly. Our system estimates the location of both the platform and APs using a SLAM-style formulation. We implement our system on DJI Matrices 100 platform, and the onboard processor is Intel NUC computer running Ubuntu Linux. The computer is equipped with a commercial Intel 5300 WiFi card and a LORD MicroStrain IMU (3DM-GX4-25). Our system could achieve the mean accuracy of 1.60 m compared with the position fused from GPS and IMU, it requires no hardware modification to the APs and no knowledge of APs' positions or fingerprint map. Only the angle of arrival extracted from CSI and IMU information are used (sect. III), and sliding window filter is used to make the metric scale observable which is similar to monocular visual-inertial fusion[14] (sect. IV).

The rest of this paper is organized as follows: Section II gives an overview of the related work. Section III presents the calculation of AoA with commercial NIC card. Section IV talks about the fusion of WiFi and IMU. Section V shows the simulation and experimental results and concludes the paper with some future work.

II. RELATED WORK

WiFi-based localization is well studied problem and a large number of methods have been proposed in recent years, which mainly could be classified into three types.

RSSI based approaches: The idea of such system is measuring the received signal strength from multiple APs which is related to the distances between the target and the APs, and solving the target's position by combining all the constraints together as a nonlinear least square problem. Since the model of RSSI depends not only on the distance but also on the environment, for example, the RSSI through the wall decades greatly, most RSSI based approaches only achieve room-level accuracy. The best known such system could achieve a median accuracy of 2-4 m[15] [16]. Additionally, the APs' positions must be known to solve the nonlinear least square problem.

Fingerprinting based approaches: This class of systems first need to collect fingerprint such as the vector of RSSIs

All authors are with the Department of Electronic and Computer Engineering, Hong Kong University of Science and Technology, Hong Kong, China. blian@connect.ust.hk, szhangaj@connect.ust.hk, eeshaojie@ust.hk

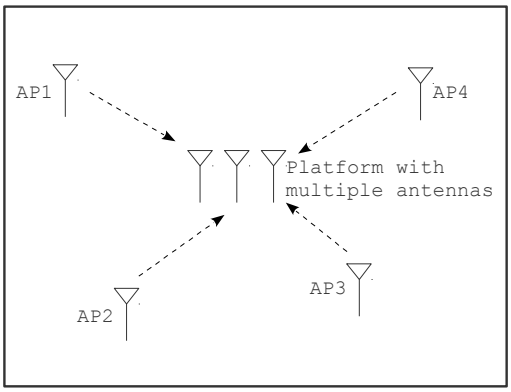

Fig. 1: System Setup

or CSIs to all APs for all the cells on the map, then could locate the target by choosing the most similar vector in the map[17] [18]. The best known system using this approach achieves the median accuracy of 0.6 m [17]. However, these systems require expensive and recurring fingerprinting operation when the environment is changed(e.g., the door is opened or the chair is moved).

AoA based approaches: After CSI-tools using Intel 5300 [19] and Atheros ar9300 [20] wireless card being released, AoA estimation has become available with commercial WiFi card and AoA based WiFi localization has become a popular research area for indoor localization. Several researchers have successfully implemented their accurate AoA based WiFi localization system using CSI information from commercial WiFi card [12] [11] [13] [21], e.g., Ubicarse [12], SpotFi [13], and Phaser [11]. Phaser could achieve median accuracy of 1 m, however, it needs to modify the hardware to combine two wireless cards with three antenna as one with five antennas. Ubicarse could achieve the median accuracy of 0.4 m without hardware modification in complex indoor environments, however, it needs the user to rotate two antennas while walking. SpotFi also could achieve comparable result as Ubicarse while it does not need to rotate the antennas and does not need additional inertial sorcerers. Unfortunately, all of these approaches above assume that the APs' positions are known in advance to locate the target.

III. CSI-BASED AOA ESTIMATION

A. CSI Measurement

It is well-known that the performance of wireless networks depends heavily on the physical layer details of the RF channel[19]. However, until 2009, only high-level information about wireless conditions like RSSI values was available from commodity 802.11 wireless card which contributes little to understanding the channel state. Fortunately, the IEEE 802.11n standard defines a mechanism for transmission of CSI between the receiver and the transmitter. Unlike the RSSI, the CSI records the signal strength and the phase information for all sub-carriers between each pair of transmitter and receiver. This standardized mechanism allows the transmitter to improve the link performance via transmit beam-forming. D. Halperin et al.[19] and Yaxiong [20] have built their tools for collecting CSI information at sub-carrier level on Intel 5300 and Atheros ar9300 wireless card respectively. A large number of researchers have successfully implemented WiFi localization system based on these tools and some of which could achieve decimeter level median accuracy.

Channel state information(CSI) is information that represents the channel's properties of a communication link with amplitude and phase, it reveals the combined effect for the wireless channel, for example, fading and scattering. To be more specifically, CSI describes how a signal propagates from the transmitter(s) to the receiver(s)[22]. In fact, the accuracy of CSI greatly influences communication performance of OFDM(Orthogonal Frequency Division Multiplexing) system.

Because electromagnetic signals superimpose on the wireless channel, we can express the propagation as a linear system:

$$\mathbf{y} = H\mathbf{x} + \mathbf{n} \tag{1}$$

where $\mathbf{x}$ is the transmitted signal, $\mathbf{y}$ is the received signal, H is the channel matrix and $\mathbf{n}$ is the noise signal.

B. AoA Estimation

To estimate the AoA of the signal from the APs, at least two antennas are required to measure the relative phase between two antennas. For simplicity, it is assumed that both the transmitter and the receivers lie on a two-dimensional plane and the signal has only single path. Suppose the AoA of the line-of-sight signal is α and the angle of the antenna array on the plane is ϕ, as illustrated in figure 2, the wireless channels measured by the receive antenna 1 and receive antenna 2 at i^{th} sub-carrier can be written as the complex number:

$$y_{1,i} = \|y_{1,i}\| e^{\frac{-j2\pi d}{\lambda_i}} x_i \tag{2}$$

$$y_{2,i} = \|y_{2,i}\| e^{\frac{-j2\pi (d - rcos(\alpha - \phi))}{\lambda_i}} x_i \tag{3}$$

where r denotes distance between two antennas, d represents the traveling distance from the transmitter to the first antenna, and λ_i is the signal wavelength of i^{th} sub-carrier. According to the IEEE 802.11n-2009 standard, the 20MHz bandwidth for each channel is divided into 64 equally spaced sub-carriers with 125KHz bandwidth. For the Intel 5300 WiFi card, only 30 sub-carriers of index $s_i = \{-28, -26, -24, -22, -20, -18, -16, -14, -12, -10, -8, -6, -4, -2, -1, 1, 3, 5, 7, 9, 11, 13, 15, 17, 19, 21, 23, 25, 27, 28\}$ are measured, and the corresponding frequencies are

$$f_i = f + s_i * 125KHz$$

where f is the central frequency of the channel.

We use λ represents the smallest wavelength for all the sub-carriers and we choose $r = \frac{\lambda}{2}$ to maximize the resolution

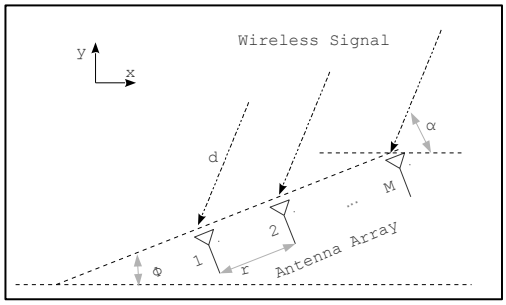

Fig. 2: Illustration of Antenna Array

of phase measurement while avoiding the phase ambiguity. Note the assumption that $d >> r$, i.e., the transmitter is far away from the receiver relative to the distance between the two antennas.

To get the equation unrelated to distance between the transmitter and receiver, we define the relative wireless channel at the i^{th} sub-carrier as, $\hat{y}_i = y_{2,i}y^*_{1,i}$, where $(.)^*$ means the complex conjugate. Mathematically, the relative channel is simplified as,

$$\hat{y}_i = y_{2,i}y^*_{1,i} = \|y_{1,i}\|\|y_{2,i}\|\|x_i\|^2 e^{\frac{j2\pi r cos(\alpha-\phi)}{\lambda}} \quad (4)$$

The phase measurement equation could be written as,

$$\angle\hat{y}_i = \psi_i = \frac{2\pi r cos(\alpha-\phi)}{\lambda_i} \quad (5)$$

where ψ_i is the measured phase of i^{th} sub-carrier. Therefore, the estimated angle is

$$\alpha = \pm \arccos(\frac{\psi_i\lambda_i}{2\pi r}) + \phi \quad (6)$$

We use the mean value of estimated AoA from all sub-carriers as the final estimation.

According to (6), there are two possible AoAs because of side ambiguity. The side ambiguity could be solved using the method used in Ubiscare [12] by rotating the antennas. We only use this method at initialization step, after that the AoA will be tracked.

IV. LINEAR SLIDING WINDOW WIFI-INERTIAL FUSION

In this section, we present an optimized-based WiFi-Inertial fusion method, which is modified from the original visual-inertial fusion framework [23] for accurate state estimation. Note that WiFi only provides AoA information, but with IMU we are able to estimate the metric position and velocity.

We consider N as the earth's inertial frame, W as the WiFi antenna frame, B as the IMU body frame, B_k as the body frame while taking k^{th} WiFi measurement. Since the IMU runs at a higher rate in our system, there are more than one IMU measurements between $\mathbf{B}_k$ and $\mathbf{B}_{k+1}$. We assume that the WiFi antenna and the IMU are pre-calibrated such that the transformation between body frame and the WiFi

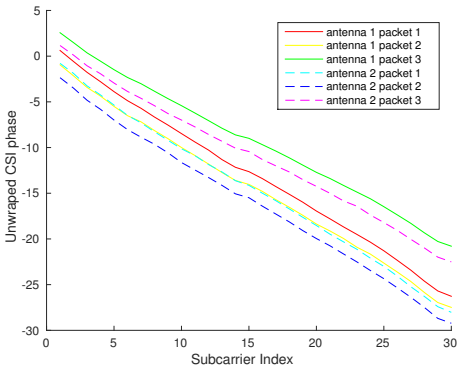

(a)

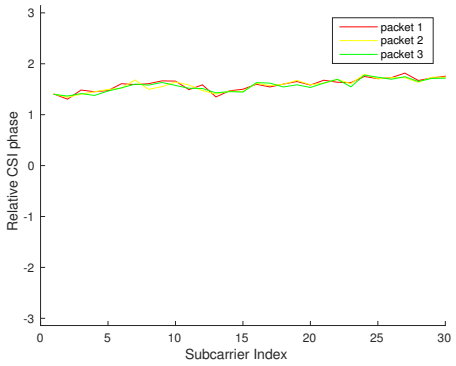

(b)

Fig. 3: CSI phase: (a) unwrapped CSI phase, (b) relative phase between antenna 1 and antenna 2. It can be seen that the phases between different sub-carriers varies greatly, but the relative phases between two antennas are very stable

antenna frame is known. $\mathbf{p}^X_Y$, $\mathbf{v}^X_Y$ and $\mathbf{R}^X_Y$ are 3D position, velocity and rotation of frame X with respect to frame Y. $\mathbf{g}^G = [0, 0, g]^T$ is the gravity vector in the earth's inertial frame, and $\mathbf{g}^X$ is the earth's gravity vector expressed in frame X.

A. Inertial Preintegration

Given more than one IMU measurements between B_k and B_{k+1}, we could summarize all these IMU measurements as one motion constrain according to Inertial Preintegration Theory [24].

The normal propagation model for position and velocity in the inertial frame can be written as,

$$\mathbf{p}^G_{B_{k+1}} = \mathbf{p}^G_{B_k} + \mathbf{v}^G_{B_k}\Delta t + \int\int_{B_k}^{B_{k+1}} (\mathbf{R}^G_B\mathbf{a}^B - \mathbf{g}^G)dt^2 \quad (7)$$

$$\mathbf{v}^G_{B_{k+1}} = \mathbf{v}^G_{B_k} + \int_{B_k}^{B_{k+1}} (\mathbf{R}^G_B\mathbf{a}^B - \mathbf{g}^G)dt \quad (8)$$

where Δt is the time difference between $\mathbf{B}_k$ and $\mathbf{B}_{k+1}$ and $\mathbf{a}^B$ is the accelerometer measurement in the body frame. It is obvious that the rotation between the inertial frame and body frame, R^G_B needs to be known in order to propagate the state with the IMU measurements. According to the

formulation in (7) and (8), if the first pose of the system is used as the reference frame, all the IMU measurements between frame B_k and B_{k+1} can be summarized as only one motion constraint, (7) and (8) can be rewritten as,

$$\mathbf{p}_{B_{k+1}}^{B_0} = \mathbf{p}_{B_k}^{B_0} + \mathbf{v}_{B_k}^{B_0}\Delta t - \mathbf{g}^{B_0}\Delta t^2/2 + \mathbf{R}_{B_k}^{B_0}\alpha_{B_{k+1}}^{B_k} \quad (9)$$

$$\mathbf{v}_{B_{k+1}}^{B_0} = \mathbf{v}_{B_k}^{B_0} - \mathbf{g}^{B_0}\Delta t + \mathbf{R}_{B_k}^{B_0}\beta_{B_{k+1}}^{B_k} \quad (10)$$

where

$$\alpha_{B_{k+1}}^{B_k} = \int\int_{B_k}^{B_{k+1}} \mathbf{R}_B^{B_k}\mathbf{a}^B\Delta t^2 \quad (11)$$

$$\beta_{B_{k+1}}^{B_k} = \int_{B_k}^{B_{k+1}} \mathbf{R}_B^{B_k}\mathbf{a}^B\Delta t \quad (12)$$

$R_{B_k}^{B_0}$ is the rotation between B_0 and B_k, which can be obtained by fusing measurements from gyroscope, magnetometer and accelerometer with Extended Kalman Filter [25]. $\alpha_{B_{k+1}}^{B_k}$ and $\beta_{B_{k+1}}^{B_k}$ can be obtained with only the IMU measurements from B_k to B_{k+1}. We can see that the constraint equations (9) and (10) for the state ($\mathbf{p}_{B_k}^{B_0}$, $\mathbf{v}_{B_k}^{B_0}$, $\mathbf{g}^{B_0}$) are all linear now.

B. Linear Sliding Window Estimator

We apply a sliding window graph-based formulation because it can accurately solve the problem in constant computation complexity. The full state parameter vector is

$$x = [\mathbf{x}_{B_0}^{B_0}, \mathbf{x}_{B_1}^{B_0}, ...\mathbf{x}_{B_N}^{B_0}, \mathbf{a}_1, \mathbf{a}_2, ...\mathbf{a}_M]$$

$$\mathbf{x}_{B_k}^{B_0} = [\mathbf{p}_{B_k}^{B_0}, \mathbf{v}_{B_k}^{B_k}, \mathbf{g}^{B_k}] \quad \text{for } k = 1, 2...N$$

$$\mathbf{p}_{B_0}^{B_0} = [0, 0, 0]$$

where $\mathbf{x}_{B_k}^{B_0}$ is the k^{th} WiFi state, N is the number of WiFi state in the sliding window, M is the number of the Access Points have been observed within the sliding window. a_l is the l^{th} Access Point's position. We keep the body frame velocity $\mathbf{v}_{B_k}^{B_k}$ and gravity vector $\mathbf{g}^{B_k}$ in the state vector to reduce the impact of rotation error on the estimation results.

Since the rotation is fixed, we can formulate the problem as a linear WiFi Inertial Navigation System by combining all measurements from both IMU and WiFi and solve the maximum likelihood estimate by minimizing the sum of the Mahalanobis norm of all measurement errors:

$$\min_{\chi}\Big\{(\mathbf{b}_p - \Lambda_p\chi) + \sum_{k\in D}\|\hat{\mathbf{z}}_{B_{k+1}}^{B_k} - \hat{\mathbf{H}}_{B_{k+1}}^{B_k}\chi\|_{\mathbf{P}_{B_{k+1}}^{B_k}}^2 + \sum_{(l,j)\in C}\|\hat{\mathbf{z}}_l^{B_j} - \hat{\mathbf{H}}_l^{B_j}\chi\|_{\mathbf{P}_l^{B_j}}^2\Big\} \quad (13)$$

where the measurements $\{\hat{\mathbf{z}}_{B_{k+1}}^{B_k}, \hat{\mathbf{H}}_{B_{k+1}}^{B_k}, \mathbf{P}_{B_{k+1}}^{B_k}\}$ and $\{\hat{\mathbf{z}}_l^{B_j}, \hat{\mathbf{H}}_l^{B_j}, \mathbf{P}_l^{B_j}\}$ are defined in sect. IV-C and sect. IV-D respectively. D is the set of all IMU measurements and C is the set of WiFi measurements between all the Access Points and WiFi states within the sliding window. $\{\mathbf{b}_p, \mathbf{\Lambda}_p\}$ is the optional prior information for the system. Since all the constraints are linear, this system can be solved by re-organizing in the following form:

$$(\mathbf{\Lambda}_p + \mathbf{\Lambda}_{imu} + \mathbf{\Lambda}_{WiFi})\chi = (\mathbf{b}_p + \mathbf{b}_{imu} + \mathbf{b}_{WiFi}) \quad (14)$$

where $\{\mathbf{\Lambda}_{imu}, \mathbf{b}_{imu}\}$ and $\{\mathbf{\Lambda}_{WiFi}, \mathbf{b}_{WiFi}\}$ are information matrices and vectors for IMU and WiFi measurements respectively.

It should be noted that since all the constraints are linear, the system in (14) has unique solution without the prior information:

$$(\mathbf{\Lambda}_{imu} + \mathbf{\Lambda}_{WiFi})\chi = (\mathbf{b}_{imu} + \mathbf{b}_{WiFi}) \quad (15)$$

To bound the computational complexity, only the latest states are kept in the state vector by removing the oldest robot state and out-of-range APs. However, if the parameters are removed from the system equations directly, some information will be lost and the scale will become unobservable using only the measurements within the sliding window. The correct way to remove the parameters is to marginalize them out, which is equivalent to Schur complement to the least square equations as described in [14] and [23].

C. IMU Measurement Model

Assume the rotation $R_{B_k}^{B_0}$is given, we can rewrite (9) and (10) as a linear function of the state χ:

$$\begin{bmatrix} \alpha_{B_{k+1}}^{B_k} \\ \beta_{B_{k+1}}^{B_k} \\ \mathbf{0} \end{bmatrix} = \begin{bmatrix} R_{B_0}^{B_k}(\mathbf{p}_{B_0}^{B_{k+1}} - \mathbf{p}_{B_0}^{B_k}) - \mathbf{v}_{B_k}^{B_k}\Delta t + \mathbf{g}^{B_k}\Delta t^2/2 \\ R_{B_0}^{B_{k+1}}\mathbf{v}_{B_{k+1}}^{B_{k+1}} - \mathbf{v}_{B_k}^{B_k} + \mathbf{g}^{B_k}\Delta t \\ R_{B_k}^{B_{k+1}}\mathbf{g}^{B_{k+1}} - \mathbf{g}^{B_k} \end{bmatrix} = H_{B_{k+1}}^{B_k}\chi \quad (16)$$

The last block line in (16) is the constraint about the gravity vector. We estimate the gravity vector for each pose in order to avoid the negative effects due to possible accumulated rotation error. All variables except the position component are independent of the accumulated rotation $R_{B_0}^{B_k}$, making them insensitive to rotation error. The linear IMU measurement model has the form:

$$\mathbf{z}_{B_{k+1}}^{B_k} \sim \mathcal{N}(\mathbf{H}_{B_{k+1}}^{B_k}\chi, \begin{bmatrix} \mathbf{P}_{B_{k+1}}^{B_k^{\alpha\beta}} & \mathbf{0} \\ \mathbf{0} & \mathbf{P}_{B_{k+1}}^{B_k^{\mathbf{g}}} \end{bmatrix}) \quad (17)$$

Note that $\alpha_{B_{k+1}}^{B_k}$ and $\beta_{B_{k+1}}^{B_k}$ are correlated since they both come from IMU measurements between B_k and B_{k+1}. The joint covariance matrix $\mathbf{P}_{B_{k+1}}^{B_k^{\alpha\beta}}$ can be calculated using the pre-integration technique proposed in [26].

D. WiFi Measurement Model

Let the l^{th} AP be the first detected in the i^{th} frame, the direction of this AP observed in the k^{th} WiFi frame, d_{kl} can be expressed as,

$$R_w^B\mathbf{d}_{kl} \sim R_{B_0}^{B_k}(\mathbf{a}_i - \mathbf{p}_{B_k}^{B_0}) \quad (18)$$

Where R_w^B is the rotation from WiFi frame to Body frame. Specially, for two-dimensional case, if the estimated AoA is α, the direction d_{kl} can be expressed as,

$$d_{kl} = [cos(\alpha), sin(\alpha), 0]^T$$

Using cross product, the constraint can be converted to linear form:

$$\lfloor R_{B_k}^{B_0} R_w^B \mathbf{d}_{kl} \rfloor_\times (\mathbf{a}_i - \mathbf{p}_{B_k}^{B_0}) = \mathbf{0} \tag{19}$$

The equation (19) can be rewritten as

$$\mathbf{0} = \lfloor R_{B_k}^{B_0} R_w^B \mathbf{d}_{kl} \rfloor_\times (\mathbf{a}_i - \mathbf{p}_{B_k}^{B_0}) = \mathbf{H}_l^{B_k} \chi \tag{20}$$

and WiFi measurement model has the form:

$$\mathbf{z}_l^{B_k} \sim \mathcal{N}(\mathbf{H}_l^{B_k} \chi, {d_l^{B_k}}^2 \bar{\mathbf{P}}_l^{B_k}) \tag{21}$$

where $d_l^{B_k}$ is the distance from the l^{th} Access Point to the B_k frame and $\bar{\mathbf{P}}_l^{B_k}$ is the WiFi observation noise. Note that $d_l^{B_k}$ is unknown initially, we initialize it with an identical value to all the measurements.

V. RESULTS

A. Simulation Result

As there is no public data with the ground truth for WiFi localization, we generate simulation data in gazebo and ROS. Four APs are placed on the ground and the platform flies as a circle pattern. The noise level of the related sensors are as follow:

TABLE I: Noise level of the simulated sensors

Sensor Type	Noise type	Noise level
gyroscope	Gaussian	0.01
accelerometer	Gaussian	0.01
angle of arrival sensor	Gaussian	0.1

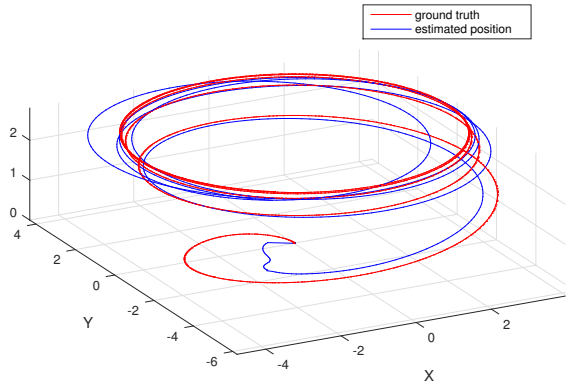

Fig. 4: Simulation result (trajectory plot)

The simulation results in figure 5 and 6 prove that the trajectory of the MAV and APs' position could be estimated simultaneously using only the IMU and the AoA measurements.

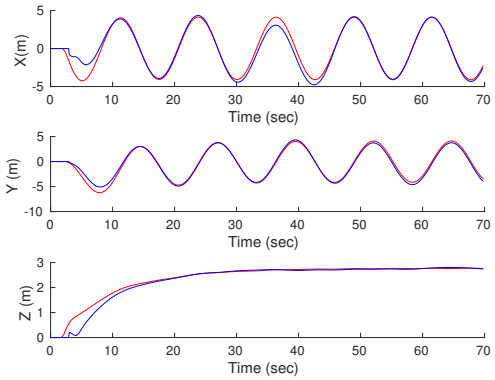

Fig. 5: Simulation result (platform position). It can be seen that the estimated platform's position will converge to the ground truth with enough motion.

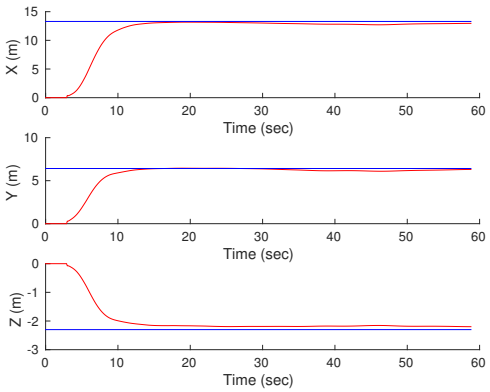

Fig. 6: Simulation result (AP position). It shows that the AP's position will converge to the ground truth with enough motion.

B. Implementation Details

We implement CWISE on an Intel NUC equipped with Intel 5300 WiFi card and a LORD MicroStrain IMU (3DM-GX4-25). We build on the 802.11n CSI tool [19] to collect the CSI information for any successfully received packets with a specialized destination MAC address. The access points work on injection mode and the receiver works on monitor mode, and all the Intel 5300 WiFi cards are configured on 5GHz channel since the phase reading on 2.4GHz always have a shift of $\frac{k\pi}{2}$. Through at most three antennas are supported for Intel 5300 WiFi card, we only use two of them because the phase reading of the third antenna is really noisy for injection/monitor mode. Specially, the wavelength $\lambda = 0.0564m$ (5.32Ghz) and the distance between two antennas $r = \frac{\lambda}{2} = 0.0282m$.

The APs are controlled by a server to broadcast the random packets one by one, there is a short interval about 2 ms between the broadcasting of different APs.

C. Experimental Results

We use an Intel NUC with Core i5 4250 processor (1.3 GHz) to compute onboard. We conduct multiple experiments

Fig. 7: Experimental Platform equipped with an Intel NUC computer, an Intel 5300 Wireless card with two antennas, and an IMU

to evaluate the performance of our system. Two APs are placed on the ground and the MAV flies at about 1 m height with a circle pattern. Currently, only two-dimensional positions are estimated because only the azimuth angle are available with two antennas. The position from GPS-IMU fusion is used as the ground truth. The standard derivation of the estimates are $\{0.998, 1.263\}$ m and the mean accuracy is 1.60 m. Since the state of the system is always unobservable without enough motion, the standard derivation is computed with the result after the first circle of flying. It should be noted that the accuracy of GPS is also meter level, the experimental results just provide an easy comparison which illustrates that our result is comparable with GPS.

The multi-path effect and non-line-of-sight Scenario is not considered in the current implementation, so the current system does not work at indoor environments and clustered environments.

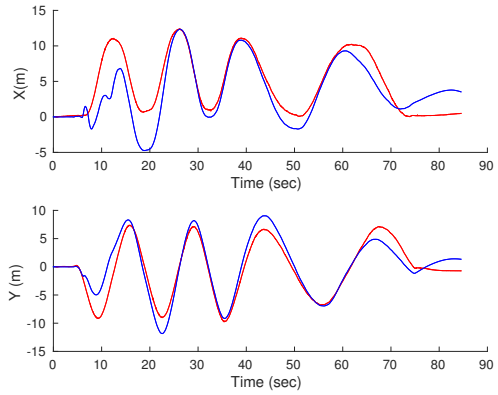

Fig. 8: Experimental result (platform position). Red lines are the positions from GPS-IMU fusion, and blue lines are the positions estimated with our method.

VI. CONCLUSIONS

In this paper, we present the first WiFi localization system with no requirement for APs' positions or fingerprint map. Our system only depends on a commercial WiFi card and an IMU. The main technical challenges are estimating the angle of arrival accurately and handling the unobservability

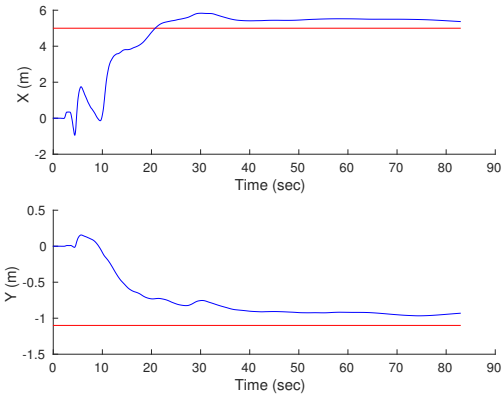

Fig. 9: Experimental result (AP position). Red lines are the ground truth of one AP's position, and blue line are the positions estimated with our method.

of the localization system. In the future, we would like to extern our localization system to three-dimensional and indoor environments.

REFERENCES

[1] A. Bachrach, S. Prentice, R. He, and N. Roy, "Range–robust autonomous navigation in gps-denied environments," *Journal of Field Robotics*, vol. 28, no. 5, pp. 644–666, 2011.

[2] S. Shen, N. Michael, and V. Kumar, "Autonomous multi-floor indoor navigation with a computationally constrained mav," in *Robotics and automation (ICRA), 2011 IEEE international conference on*, pp. 20–25, IEEE, 2011.

[3] F. Fraundorfer, L. Heng, D. Honegger, G. H. Lee, L. Meier, P. Tanskanen, and M. Pollefeys, "Vision-based autonomous mapping and exploration using a quadrotor mav," in *Intelligent Robots and Systems (IROS), 2012 IEEE/RSJ International Conference on*, pp. 4557–4564, IEEE, 2012.

[4] K. Schmid, T. Tomic, F. Ruess, H. Hirschmuller, and M. Suppa, "Stereo vision based indoor/outdoor navigation for flying robots," in *Intelligent Robots and Systems (IROS), 2013 IEEE/RSJ International Conference on*, pp. 3955–3962, IEEE, 2013.

[5] S. Weiss, M. W. Achtelik, S. Lynen, M. Chli, and R. Siegwart, "Real-time onboard visual-inertial state estimation and self-calibration of mavs in unknown environments," in *Robotics and Automation (ICRA), 2012 IEEE International Conference on*, pp. 957–964, IEEE, 2012.

[6] D. G. Kottas, J. A. Hesch, S. L. Bowman, and S. I. Roumeliotis, "On the consistency of vision-aided inertial navigation," in *Experimental Robotics*, pp. 303–317, Springer, 2013.

[7] R. Mur-Artal, J. Montiel, and J. D. Tardos, "Orb-slam: a versatile and accurate monocular slam system," *Robotics, IEEE Transactions on*, vol. 31, no. 5, pp. 1147–1163, 2015.

[8] A. S. Huang, A. Bachrach, P. Henry, M. Krainin, D. Maturana, D. Fox, and N. Roy, "Visual odometry and mapping for autonomous flight using an rgb-d camera," in *International Symposium on Robotics Research (ISRR)*, vol. 2, 2011.

[9] B. Ferris, D. Fox, and N. D. Lawrence, "Wifi-slam using gaussian process latent variable models.," in *IJCAI*, vol. 7, pp. 2480–2485, 2007.

[10] J. Xiong and K. Jamieson, "Arraytrack: a fine-grained indoor location system," in *Presented as part of the 10th USENIX Symposium on Networked Systems Design and Implementation (NSDI 13)*, pp. 71–84, 2013.

[11] J. Gjengset, J. Xiong, G. McPhillips, and K. Jamieson, "Phaser: enabling phased array signal processing on commodity wifi access points," in *Proceedings of the 20th annual international conference on Mobile computing and networking*, pp. 153–164, ACM, 2014.

[12] S. Kumar, S. Gil, D. Katabi, and D. Rus, "Accurate indoor localization with zero start-up cost," in *Proceedings of the 20th annual international conference on Mobile computing and networking*, pp. 483–494, ACM, 2014.

[13] M. Kotaru, K. Joshi, D. Bharadia, and S. Katti, "Spotfi: Decimeter level localization using wifi," in *Proceedings of the 2015 ACM Conference on Special Interest Group on Data Communication*, pp. 269–282, ACM, 2015.

[14] G. Sibley, L. Matthies, and G. Sukhatme, "Sliding window filter with application to planetary landing," *Journal of Field Robotics*, vol. 27, no. 5, pp. 587–608, 2010.

[15] P. Bahl and V. N. Padmanabhan, "Radar: An in-building rf-based user location and tracking system," in *INFOCOM 2000. Nineteenth Annual Joint Conference of the IEEE Computer and Communications Societies. Proceedings. IEEE*, vol. 2, pp. 775–784, Ieee, 2000.

[16] K. Chintalapudi, A. Padmanabha Iyer, and V. N. Padmanabhan, "Indoor localization without the pain," in *Proceedings of the sixteenth annual international conference on Mobile computing and networking*, pp. 173–184, ACM, 2010.

[17] M. Youssef and A. Agrawala, "The horus wlan location determination system," in *Proceedings of the 3rd international conference on Mobile systems, applications, and services*, pp. 205–218, ACM, 2005.

[18] X. Wang, L. Gao, S. Mao, and S. Pandey, "Deepfi: Deep learning for indoor fingerprinting using channel state information," in *Wireless Communications and Networking Conference (WCNC), 2015 IEEE*, pp. 1666–1671, IEEE, 2015.

[19] D. Halperin, W. Hu, A. Sheth, and D. Wetherall, "Tool release: gathering 802.11 n traces with channel state information," *ACM SIGCOMM Computer Communication Review*, vol. 41, no. 1, pp. 53–53, 2011.

[20] Z. Li, Y. Xie, M. Li, and K. Jamieson, "Recitation: Rehearsing wireless packet reception in software," in *Proceedings of the 21st Annual International Conference on Mobile Computing and Networking*, pp. 291–303, ACM, 2015.

[21] S. Kumar, E. Hamed, D. Katabi, and L. Erran Li, "Lte radio analytics made easy and accessible," in *ACM SIGCOMM Computer Communication Review*, vol. 44, pp. 211–222, ACM, 2014.

[22] K. Wu, J. Xiao, Y. Yi, M. Gao, and L. M. Ni, "Fila: Fine-grained indoor localization," in *INFOCOM, 2012 Proceedings IEEE*, pp. 2210–2218, IEEE, 2012.

[23] S. Shen, Y. Mulgaonkar, N. Michael, and V. Kumar, "Initialization-free monocular visual-inertial state estimation with application to autonomous mavs," in *Experimental Robotics*, pp. 211–227, Springer, 2016.

[24] T. Lupton and S. Sukkarieh, "Visual-inertial-aided navigation for high-dynamic motion in built environments without initial conditions," *Robotics, IEEE Transactions on*, vol. 28, no. 1, pp. 61–76, 2012.

[25] N. Trawny and S. I. Roumeliotis, "Indirect kalman filter for 3d attitude estimation," *University of Minnesota, Dept. of Comp. Sci. & Eng., Tech. Rep*, vol. 2, p. 2005, 2005.

[26] C. Forster, L. Carlone, F. Dellaert, and D. Scaramuzza, "Imu preintegration on manifold for efficient visual-inertial maximum-a-posteriori estimation," in *Robotics: Science and Systems XI*, no. EPFL-CONF-214687, 2015.